GENERALIZATION OF THE SPLIT FLOW HEAT EXCHANGER GEOMETRY FOR ENHANCED HEAT TRANSFER

Governing equations for heat transfer in a split flow heat exchanger with four tube passes are dervied. Using these equations, curves for Logarithmic Mean Temperature Difference correction factor, and temperature efficiency, heretofore unavailable in the literature, are presented. Study of salient characteristics of the heat transfer process in a typical example problem points to possible strategies for optimization of the split flow geometry for increased heat transfer.

Krishna P. Singh
President & CEO
Holtec International
Marlton, NJ
and
Michael J. Holtz

1. INTRODUCTION

Split Flow Heat Exchangers (Fig. 1), referred to as the "G-type" in the TEMA standards [1], are quite popular with heat exchanger designers for several reasons. One important reason is their ability to produce "temperature correction factors" comparable to those in a F-type shell (TEMA designation for two-pass shell) with only a fraction of the shellside pressure loss in the latter type. Despite the popularity of the split flow construction, it is somewhat odd that a consistent heat transfer analysis for the "split 4" (split flow shell-4 tube pass) geometry (See Fig. 1) does not exist in the open literature. Presumably, the lack of appropriate treatment of this configuration is due to the relative complexity of the governing equations which make derivation of analytical expressions quite tedius.

Working charts for the temperature correction factor by treating the split-4 exchanger as two "divided flow two tube pass shells" in series were first proposed by Gulley [2]. Gulley's model, though theoretically imprecise, gives reasonably reliable values of temperature correction factor for most of the working range. However, the necessity of having design data based on the true model of the "split-4" construction is undeniably important; perhaps long overdue.

This consideration prompted us to develop the governing equations to determine the temperature correction factor in terms of the well known duo of parameters; temperature efficiency P, and thermal flow rate ratio, R.[1, P144]. Furthermore, the "temperature efficiency" is plotted as a function of the "reduced thermal flux", $\psi(\psi = UA^*/W_tC_t)$ with the "thermal flow rate ratio" as the parameter. These two sets of curves enable complete characterization of heat transfer in a split flow heat exchanger with four tube passes.

0065-8812-79-2792-0189-$00.95.

Finally, temperature profiles of shell and tubeside streams for a typical commercial "split-4" heat exchanger are shown to illustrate hidden built-in inefficiencies in exchangers of this construction. The shape of the temperature curves suggest design modifications which are discussed in some detail in Section 4.

To fix ideas, it is appropriate to outline the major assumptions made in this analysis. These are:

a. Complete mixing is supposed to take place at all locations in the shell; i.e. no stratification, bypass, etc.

b. The shell fluid is assumed to undergo negligible temperature change in any single baffle spacing in crossflow.

c. The specific heats of both heat exchanging fluids are constant

d. No phase change in either fluid

e. Negligible heat loss from the system

f. No heat or mass transfer across the pass partition plates, longitudinal baffle, etc.

g. Steady state conditions

h. Piecewise constant heat transfer coefficient: The heat exchanger is subdivided into four subregions (Fig. 2). The heat transfer coefficient is assumed to be constant in each subregion, however it can be different from one subregion to another.

The four subregions are shown in Figure 2. In the following formulation, the shellside flow rate, W_i and surface area A_i are also allowed to be unequal in the four subregions. The full implication of this feature will become clear later in this paper. At this point it suffices to say that these features permit complete generalizations of the "Split-4" geometry; and added insight into the heat transfer process.

The assumptions described in the foregoing seek to idealize the physical problem to render it amenable to engineering analysis. In reality, of course, none of the above assumptions hold rigorously. Their relative influence in introducing error in the results of the analysis has been subject to great interest in recent years [3,4]. The findings in the above referenced investigations are reassuring to the designer who cannot commit the time or resources for a rigorous study.

We will next derive the governing heat transfer equations.

2. FORMULATION

a. Governing Equations:

Figure 2 shows a schematic representation of the heat transfer process in a "split-4" heat exchanger. The heat transfer region is subdivided into four subregions, each consisting of one shell pass (unidirectional shell flow) and two tube passes. The shell fluid exit temperature from subregion i is labeled as θ_i^*. The temperature of shellside fluid at a generic location in subregion i is denoted by ξ_i^*, and the corresponding tubeside fluid temperatures in the two passes are denoted by α_{i1}^* and α_{i2}^*, respectively. Second subscript is 1 for the tube leg cocurrent with the shell stream and 2 for the tube leg countercurrent to the shell stream. This notation is illustrated for all 4 subregions in Figure 2. Further, the origin of the coordinate system for each subregion is set at the location where the shellside stream enters that subregion. For convenience we will use tube outer heat transfer surface area A^* as the generalized independent coordinate parameter.

Note, with above notation, at the interface of subregions 1 and 2 (A=0), continuity of tubeside fluid temperatures in each tube-pass requires

$$\alpha_{11}^* = \alpha_{22}^*$$
$$\alpha_{12}^* = \alpha_{21}^*$$

The equations for continuity of heat transfer across an elemental tube surface dA (Surface area of all tubes in one pass in an incremented tube length) can be written:

$$-W_i\, C_s\, d\xi_i^* = W_t\, C_t\, (d\alpha_{i1}^* - d\alpha_{i2}^*) \qquad (1)$$

$$-W_i\, C_s\, d\xi_i^* = U_i\, dA\, (2\xi_i^* - \alpha_{i1}^* - \alpha_{i2}^*) \qquad (2)$$

$$W_t\, C_t\, d\alpha_{i1}^* = U_i\, dA\, (\xi_i^* - \alpha_{i1}^*) \qquad (3)$$

$$-W_t\, C_t\, d\alpha_{i2}^* = U_i\, dA\, (\xi_i^* - \alpha_{i2}^*) \qquad (4)$$

where i = 1,...4 for the four subregions,

Thus,

$$\frac{d\alpha_{i1}^*}{dA} + \frac{d\alpha_{i2}^*}{dA} = \frac{U_i}{W_t\, C_t}\,(\alpha_{i2}^* - \alpha_{i1}^*) \qquad (5)$$

We seek to eliminate α^*_{i1} and α^*_{i2} from Eq. (2). Differentiating Eq. (2) with respect to A yields,

$$\frac{d^2\xi_i^*}{dA^2} = \frac{-U_i}{W_i C_s}\left[2\frac{d\xi_i^*}{dA} - \left(\frac{d\alpha^*_{i1}}{dA} + \frac{d\alpha^*_{i2}}{dA}\right)\right]$$

This, in conjunction with Eq. (5) yields,

$$\frac{d^2\xi_i^*}{dA^2} = \frac{-U_i}{W_i C_s}\left[2\frac{d\xi_i^*}{dA} - \frac{U_i}{W_t C_t}(\alpha^*_{i2} - \alpha^*_{i1})\right]$$

Differentiating above equation, and utilizing Eq.(1), a third order differential equation in ξ_i^* is obtained

$$\frac{d^3\xi_i^*}{dA^3} + \frac{2U_i}{W_i C_s}\frac{d^2\xi_i^*}{dA^2} - \frac{U_i^2}{W_t^2 C_t^2}\frac{d\xi_i^*}{dA} = 0 \quad (6)$$

Let us introduce a dimensionless independent variable χ where

$$\chi = \frac{A}{A^*} \quad (7)$$

Similarly, let $\xi_i = \xi_i^*/(T_1 - t_1)$ and

$$\alpha_{ij} = \alpha^*_{ij}/(T_1 - t_1) \quad (7.a)$$

Denoting $\frac{d}{d\chi}$ with ′ (prime), we have

$$\xi_i''' + \frac{2U_iA^*}{W_iC_s}\xi_i'' - \frac{U_i^2A^{*2}}{W_t^2C_t^2}\xi_i' = 0 \quad (8)$$

or $$\xi_i''' + 4\gamma_i R_i \xi_i'' - \gamma_i^2 \xi_i' = 0 \quad (9)$$

where, $$\frac{U_iA^*}{W_tC_t} = \gamma_i \quad (10)$$

$$\frac{W_tC_t}{2W_iC_s} = R_i \quad (11)$$

Solution of Eq. (9) is given in terms of 3 arbitrary constants (for each subregion)

$$\xi_i = B_i + C_i e^{m_i\chi} + D_i e^{n_i\chi} \quad i = 1,\ldots 4 \quad (12)$$

where

$$m_i = \gamma_i\left[-2R_i + (1 + 4R_i^2)^{1/2}\right]$$
$$n_i = \gamma_i\left[-2R_i - (1 + 4R_i^2)^{1/2}\right] \quad (13)$$

Twelve constants of integration, B_i, C_i, D_i, (i = 1,...4) are to be evaluated using the appropriate boundary and interface conditions.

Before proceeding to set up the initial and boundary conditions, it is useful to define α_{i1} and α_{i2} in terms of ξ_i and its derivatives. We note, from Eq. (2)

$$\alpha^*_{i1} + \alpha^*_{i2} = 2\xi_i^* + \frac{W_iC_s}{U_i}\frac{d\xi_i^*}{dA} \quad (14)$$

Furthermore, rewriting Eq. (5), we have

$$\alpha^*_{i2} - \alpha^*_{i1} = \frac{W_tC_t}{U_i}\left(\frac{d\alpha_{i2}}{dA} + \frac{d\alpha_{i1}}{dA}\right)$$

or $$\alpha^*_{i2} - \alpha^*_{i1} = \frac{W_tC_t}{U_i}\left[\frac{2d\xi_i^*}{dA} + \frac{W_iC_s}{U_i}\frac{d^2\xi_i^*}{dA^2}\right] \quad (15)$$

Eqs. (14) and (15) yield the desired expressions for α^*_{i1} and α^*_{i2}. We have

$$\alpha^*_{i1} = \frac{-W_iC_sW_tC_t}{2U_i^2}\frac{d^2\xi_i^*}{dA^2} + \left[\frac{W_iC_s}{2U_i} - \frac{W_tC_t}{U_i}\right]\frac{d\xi_i^*}{dA} + \xi_i^*$$

$$\alpha^*_{i2} = \frac{W_iC_sW_tC_t}{2U_i^2}\frac{d^2\xi_i^*}{dA^2} + \left[\frac{W_iC_s}{2U_i} + \frac{W_tC_t}{U_i}\right]\frac{d\xi_i^*}{dA} + \xi_i^* \quad (16)$$

Or, in terms of previously defined dimensionless quantities,

$$\alpha_{i1} = \frac{-1}{4R_i\gamma_i^2}\xi_i''' + \frac{1}{\gamma_i}\left(\frac{1}{4R_i} - 1\right)\xi_i' + \xi_i \quad (17)$$

$$\alpha_{i2} = \frac{1}{4R_i\gamma_i^2}\xi_i''' + \frac{1}{\gamma_i}\left(1 + \frac{1}{4R_i}\right)\xi_i' + \xi_i \quad (18)$$

Similarly

$$\alpha_{i1} + \alpha_{i2} = 2\xi_i + \frac{1}{2R_i\gamma_i}\xi_i' \quad (19)$$

$$\alpha_{i2} - \alpha_{i1} = \frac{1}{\gamma_i}\left(2\xi_i' + \frac{1}{2R_i\gamma_i}\xi''\right) \quad (20)$$

Finally, derivatives of ξ_i follow directly from Eq. (12)

$$\xi_i' = m_iC_ie^{m_i\chi} + n_iD_ie^{n_i\chi} \quad (21)$$

$$\xi_i'' = m_i^2C_ie^{m_i\chi} + n_i^2D_ie^{n_i\chi} \quad (22)$$

Thus

$$\alpha_{ij} = \frac{\delta_j}{4R_i\gamma_i^2}\xi_i''' + \frac{\delta_j}{\gamma_i}\left(1 + \frac{\delta_j}{4R_i}\right)\xi_i' + \xi_i; \quad j = 1, 2$$

where

$$\delta_j = -1 \text{ for } j = 1$$
$$= 1 \text{ for } j = 2$$

Substituting for the derivatives of ξ_i from Eqs. (12), (21) and (22), and gathering terms, we have

$$\alpha_{ij} = B_i + C_i e^{m_i X} \{1 + \frac{m_i \delta_j}{\gamma_i}(1 + \frac{\delta_j}{4R_i}) + \frac{m_i^2 \delta_j}{4R_i \gamma_i^2}\} + D_i e^{n_i X} \{1 + \frac{n_i \delta_j}{\gamma_i} (1 + \frac{\delta_j}{4R_i} + \frac{n_i^2 \delta_j}{4R_i \gamma_i^2})\}$$
$$i = 1, 4; \qquad j = 1, 2 \qquad (23)$$

Similarly

$$\alpha_{i2} + \alpha_{i1} = 2B_i + C_i e^{m_i X} (2 + \frac{m_i}{2R_i \gamma_i}) + D_i e^{n_i X} (2 + \frac{n_i}{2R_i \gamma_i}); \; i = 1, 4 \qquad (24)$$

$$\alpha_{i2} - \alpha_{i1} = C_i e^{m_i X} (\frac{2m_i}{\gamma_i} + \frac{m_i^2}{2R_i \gamma_i^2}) + D_i e^{n_i X} (\frac{2n_i}{\gamma_i} + \frac{n_j}{2\gamma_i^2 R_i}) \qquad (25)$$

b. Boundary Conditions

12 constants of integration (B_i, C_i, D_i; $i = 1,\ldots 4$) are computed by solving twelve simultaneous equations. Of these, ten equations follow from interface temperature continuity requirements, and the remaining two from the imput temperature data. Let us assume for now that T_1 and t_1 are the specified temperatures. Our object now is to find the outlet temperatures T_2 and t_2 (and thus implicitly, the heat duty). Surface areas A_i and corresponding heat transfer coefficient U_i and assumed to be given. The following relationships are immediately evident:

(i) Interface conditions:

$$\alpha_{11} + \alpha_{12} = \alpha_{22} + \alpha_{21} \; @ \; X_1 = X_2 = 0 \quad (a)$$

$$\alpha_{11} - \alpha_{12} = \alpha_{22} - \alpha_{21} \; @ \; X_1 = X_2 = 0 \quad (b)$$

$$\alpha_{21} - \alpha_{22} = 0 \; @ \; (X = X_2) \quad (c)$$

$$\alpha_{12} \; @ \; (X = X_1) = \alpha_{32} \; @ \; X = 0 \quad (d) \qquad (26)$$

$$(\alpha_{31} + \alpha_{32}) \; @ \; (X = X_3) = (\alpha_{42} + \alpha_{41}) @ X = X_4 \quad (e)$$

$$(\alpha_{31} - \alpha_{32}) \; @ \; (X = X_3) = (\alpha_{42} - \alpha_{41}) @ X = X_4 \quad (f)$$

$$\alpha_{41} - \alpha_{42} = 0 @ \; X = 0 \quad (g)$$

$$\xi_1 @ \; (X = X_1) = \xi_3 \; @ \; X = 0 \quad (h)$$

$$\xi_2 @ \; (X = X_2) = \xi_4 \; @ \; X = 0 \quad (i)$$

$$\xi_1 = \xi_2 \; @ \; X = 0 \quad (j)$$

These ten equations in conjunction with Eqs. (23) - (25) yield 10 linear algebraic equations in the undetermined constants B_i, C_i, D_i ($i = 1, 2, 3, 4$). These equations are independent of input data. Finally, two additional equations are obtained by appealing to the prescribed initial conditions. Thus, if T_1 and t_1 are specified, we have

$$\xi_1 \Big|_{X=0} - \alpha_{31} \Big|_{X=0} = 1 \qquad (k)$$

$$\xi_1 \Big|_{X=0} + \alpha_{31} \Big|_{X=0} = \frac{T_1 + t_1}{T_1 - t_1} \qquad (\ell)$$

It is to be noted that we used $(T_1 - t_1)$ as the non-dimensionalizing parameter (Eq. 7.a) since T_1 and t_1 are assumed to be known. If, for example, T_1 and t_2 were specified in the physical problem, then one would use $(T_1 - t_2)$ as the non-dimensionalizer, and equations (k) and (ℓ) will be accordingly changed.

In this manner, twelve linear algebraic equations in twelve unknowns are unknowns compiled. This may be written in the subscript notation as

$$M_{ij} X_j = f_i; \; i, j = 1, 2....12 \qquad (27)$$

where the equivalence

$\{X_1 \; X_2 \ldots\ldots X_{11}, X_{12}\} = \{B_1, C_1, D_1, B_2, C_2, D_2, B_3, C_3, D_3, B_4, C_4, D_4\}$ is implied. $f_i = 0$ for $i = 1, 10$. $f_{11} = 1$, $f_{12} = \frac{T_1 + t_1}{T_1 - t_1}$

f_{12} will be differently specified if T_1 and t_1 are not the specified data in the problem. The non-zero coefficients of {M} matrix are given in the appendix.

3. DESIGN CHARTS

Utilizing the formulation developed in the preceding section, curves for the "LMTD correction factor" as a function of temperature efficiency P, and thermal flow rate ratio R are developed. The temperature efficiency, P, in Fig. 3 is defined as

$$P = \frac{t_2 - t_1}{T_1 - t_1} \qquad (28)$$

Similarly, the thermal flow rate ratio R is defined as

$$R = W_t C_t / W_s C_s \qquad (29)$$

where W_s is the total shellside flow rate, i.e.

$$W_s = W_1 + W_2 = W_3 + W_4$$

The curves for temperature efficiency P in terms of R, and reduced thermal flux ψ, are also produced (Fig.4). These two charts completely characterize the gross heat transfer behavior of G shell-4 tube pass heat exchangers.

Extensive numerical tests showed P is exclusively a function of R and ψ. This implies that the LMTD correction factor F is strictly a function of ψ and R. Since ψ and R do not contain terminal point temperatures in their definitions, it follows that F is independent of terminal point temperatures. These facts are very helpful in predicting exchanger response to variation in input temperatures. For example, if the exchanger performance (heat duty, P, F etc) are known for the design point, then the outlet temperatures corresponding to another set of inlet temperatures (T_1 and t_1) can be immediately computed using Eq. (28), and heat balance relationships.

Having established the relationship between vital dimensionless quantities (ψ and R) central to the performance of G-shell 4-tube pass exchangers, we now proceed to study a typical problem in some detail.

4. DISCUSSION

To examine the temperature profiles inside the "split-4" heat exchanger, the following example problem is considered:

a. Tubeside data
W_t = 181437 kg/hr (400,000 #/hr)
t_1 = 26.7°c (80°F)
C_t = 4186 J/kg-K. (1.0 BTU/#-°F)

b. Shellside data
$W_1 = W_2$ = 90719 kg/hr (200,000#/hr)
C_s = 4186 J/kg-K (1.0 BTU/#-°F)
T_1 = 37.78°c (100°F)

c. Performance data
$U_1 = U_2 = U_3 = U_4$ = 2271 J/m^2-s-K
(400 BTU/hr-sq.ft.-oF)

$2A_1 = 2A_2 = 2A_3 = 2A_4$ = 90.29 sq. m (1000 sq.ft)

The LMTD correction factor is computed to be 0.614. The temperature profiles (dimensionless) of the shell and tubeside streams are shown in Fig. 5. It is interesting to observe that in some portions of the heat transfer surface "reverse heat transfer" takes place (hatched region in the figure). This is clearly undesirable. The shape of the temperature curves in Figure 5 indicates that shifting the central axis somewhat to the left might reduce or even eliminate the reverse heat transfer segment. Our preliminary calculations show that this is indeed true. Moving the shell inlet (and outlet) nozzle to the left of center augments overall heat duty. Of course, setting nozzles off-center results in unequal subdivision of flow rates. The subdivision of flow rates can be further modified by changing baffle spacings, cut overlaps, etc. in the four subregions. Thus two distinct techniques to improve heat transfer in a G-type shell can be identified:

(i) Uneven flow
(ii) Unequal heat transfer area

Detailed results on the impact of these techniques in boosting heat transfer are not presented here for lack of time. However, the formulation given in this paper will enable a complete optimization study. Such a study is currently underway.

Asymmetric nozzle location to improve heat transfer is not peculiar to the split flow heat exchangers. Singh [5] has recently derived an analytical expression to determine the optimal location of single shell nozzle (vis-a-vis the double nozzle at the opposite end) to maximize heat transfer in a divided flow (TEMA type J) one tube pass heat exchanger. At least in these two cases studied to date, nature seems to repudiate symmetry.

APPENDIX

Coefficients of {M} Matrix

$M(1,1) = 2$; $M(1,2) = \omega_1$; $M(1,3) = \Omega_1$

$M(1,4) = -2$; $M(1,5) = -\omega_2$; $M(1,6) = -\Omega_2$

$M(2,2) = \frac{m_1\omega_1}{\gamma_1}$; $M(2,3) = \frac{n_1\Omega_1}{\gamma_1}$

$M(2,5) = \frac{m_2\omega_2}{\gamma_2}$; $M(2,6) = \frac{n_2\Omega_2}{\gamma_2}$

$M(3,5) = \phi_2(\lambda_{21} - \lambda_{22})$; $M(3,6) = \psi_2(\Lambda_{21} - \Lambda_{22})$

$M(4,1) = 1$; $M(4,2) = \lambda_{12}\phi_1$; $M(4,3) = \Lambda_{12}\psi_1$

$M(4,7) = -1$; $M(4,8) = -\lambda_{32}$; $M(4,9) = -\Lambda_{32}$

$M(5,7) = 2$; $M(5,8) = \phi_3\omega_3$; $M(5,9) = \Omega_3\psi_3$

$M(5,10) = -2$; $M(5,11) = -\phi_4\omega_4$; $M(5,12) = -\Omega_4\psi_4$

$M(6,8) = \frac{m_3\phi_3\omega_3}{\gamma_3}$; $M(6,9) = \frac{n_3\psi_3\Omega_3}{\gamma_3}$

$M(6,11) = \frac{m_4\phi_4\omega_4}{\gamma_4}$; $M(6,12) = \frac{n_4\psi_4\Omega_4}{\gamma_4}$

$M(7,11) = \lambda_{41} - \lambda_{42}$; $M(7,12) = \Lambda_{41} - \Lambda_{42}$

$M(8,1) = 1$; $M(8,2) = \phi_1$; $M(8,3) = \psi_1$

$M(8,7) = -1$; $M(8,8) = -1$; $M(8,9) = -1$

$M(9,4) = 1$; $M(9,5) = \phi_2$; $M(9,6) = \psi_2$

$M(9,10) = M(9,11) = M(9,12) = -1$

$M(10,1) = M(10,2) = M(10,3) = 1$

$M(10,4) = M(10,5) = M(10,6) = -1$

$M(11,1) = M(11,2) = M(11,3) = 1$

$M(11,7) = -1$; $M(11,8) = -\lambda_{31}$, $M(11,9) = -\Lambda_{31}$

$M(12,1) = M(12,2) = M(12,3) = 1$

$M(12,7) = 1$; $M(12,8) = \lambda_{31}$, $M(12,9) = \Lambda_{31}$

In the foregoing term definitions, the following notations are used

$$\omega_i = 2 + \frac{m_i}{2\gamma_i R_i}$$

$$\Omega_i = 2 + \frac{n_i}{2\gamma_i R_i}$$

$$\phi_i = e^{m_i X_i}$$

$$\psi_i = e^{n_i X_i}$$

$$\lambda_{ij} = 1 + \frac{m_i\delta_j}{\gamma_i}\left(1 + \frac{\delta_j}{4R_i}\right) + \frac{m_i^2\delta_j}{4\gamma_i^2 R_i}$$

$$\Lambda_{ij} = 1 + \frac{n_i\delta_j}{\gamma_i}\left(1 + \frac{\delta_j}{4R_i}\right) + \frac{n_i^2\delta_j}{4\gamma_i^2 R_i}$$

NOTATION

A^*	–	Overall heat transfer surface area on tube outside surface.
A	–	Generic Surface Area (independent Coordinate)
A_i	–	Heat transfer surface area in subregion i in one tube pass
C_s	–	Specific heat of shellside fluid at its average bulk temperature.
C_t	–	Specific heat of tubeside fluid at its average bulk temperature
$\{f\}$	–	RHS Vector
$[M]$	–	Coefficient matrix
P	–	Temperature efficiency
R	–	Thermal flow rate ratio = $W_t C_t / ((W_1 + W_2) C_s)$
R_i	–	Ratio of thermal flow rates, dimensionless (Eq. 11)
T_1	–	Shell side inlet temperature
t_1	–	Tubeside inlet temperature
T_2	–	Shell outlet temperatures
t_2	–	Tube outlet temperatures
U	–	Average heat transfer coefficient
U_i	–	Overall heat transfer coefficient in subregion i
W_t	–	Flow rate of tubeside fluid
W_i	–	Flow rate of shell side fluid in subregion i
α^*_{ij}	–	Temperature of tubeside fluid in leg j (j = 1,2) in subregion i at a generic point.
γ_i	–	Dimensionless Thermal flux in region i (Eq.10)

ξ_i^* - Temperature of shellside fluid in subregion i at a generic point.

ψ - Reduced thermal flux (= UA^*/W_tC_t)

X_i - Dimensionless surface area corresponding to A_i

X - Dimensionless surface area coordinate (Eq.7)

θ_i^* - Temperature of shellside fluid exiting subregion i

Superscript:
*Denotes a dimensioned quantity. Its dimensionless counterpart is indicated without a "star" superscript.

Literature Cited

[1] "Standards of Tubular Manufacturers Association", sixth edition, New York (1978)

[2] Gulley, D. L., "How to Figure True Temperature Difference in Shell-and-Tube Exchangers", The Oil and Gas Journal, Sept.14,1964; pp108 to 114.

[3] Gardner, K. A. and Taborek, J., "Mean Temperature Difference: A Reappraisal", AICHE Journal, Vol. 23, Nov.6, 1977, pp 777 to 786

[4] Kao, S., "Analysis of Multipass Heat Exchangers with Variable Properties and Transfer Rate", Trans. ASME. Journal of Heat Transfer, 1975, pp 509 to 515.

[5] Singh, K. P., "Heat Transfer Characteristics of a Generalized Divided Flow Heat Exchangers", to be presented at the Conference on Industrial Energy Conservation Technology, Houston, April 25 to 29, 1979 (to be published in the proceedings).

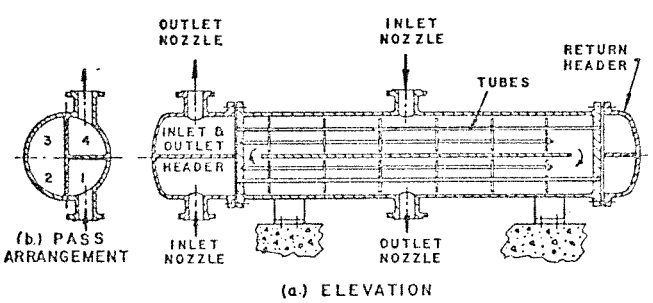

Fig. 1. 4-tube pass split flow heat exchanger.

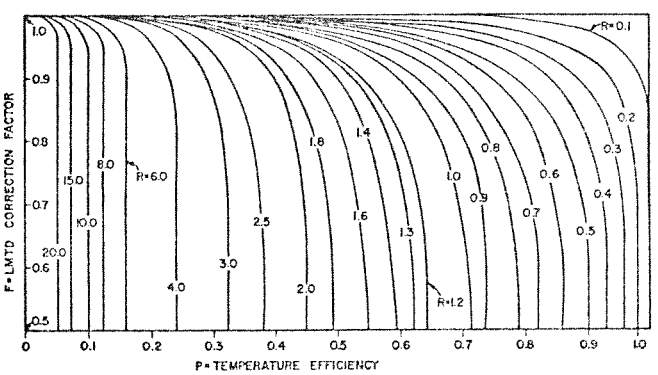

Fig. 3. Temperature correction factor for split flow-four tube pass heat exchanger.

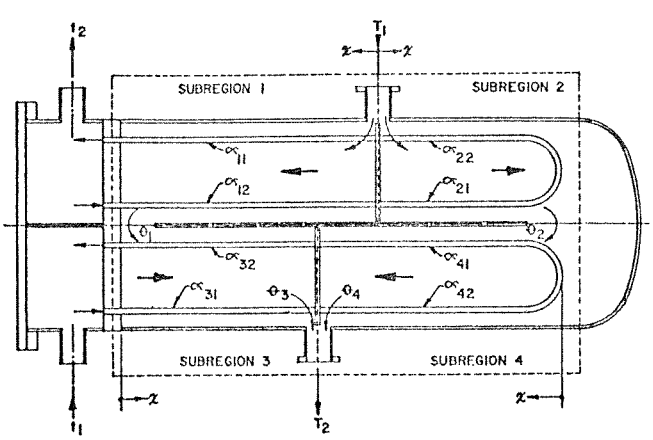

Fig. 2. Thermal subregions for "split 4" geometry.

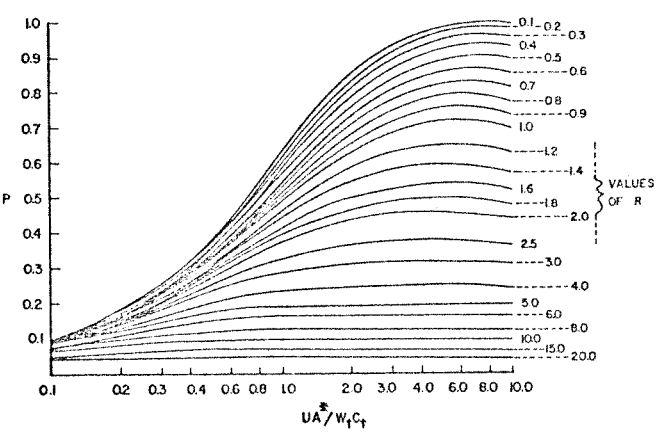

Fig. 4. Temperature efficiency curves for split flow—four tube pass heat exchanger.

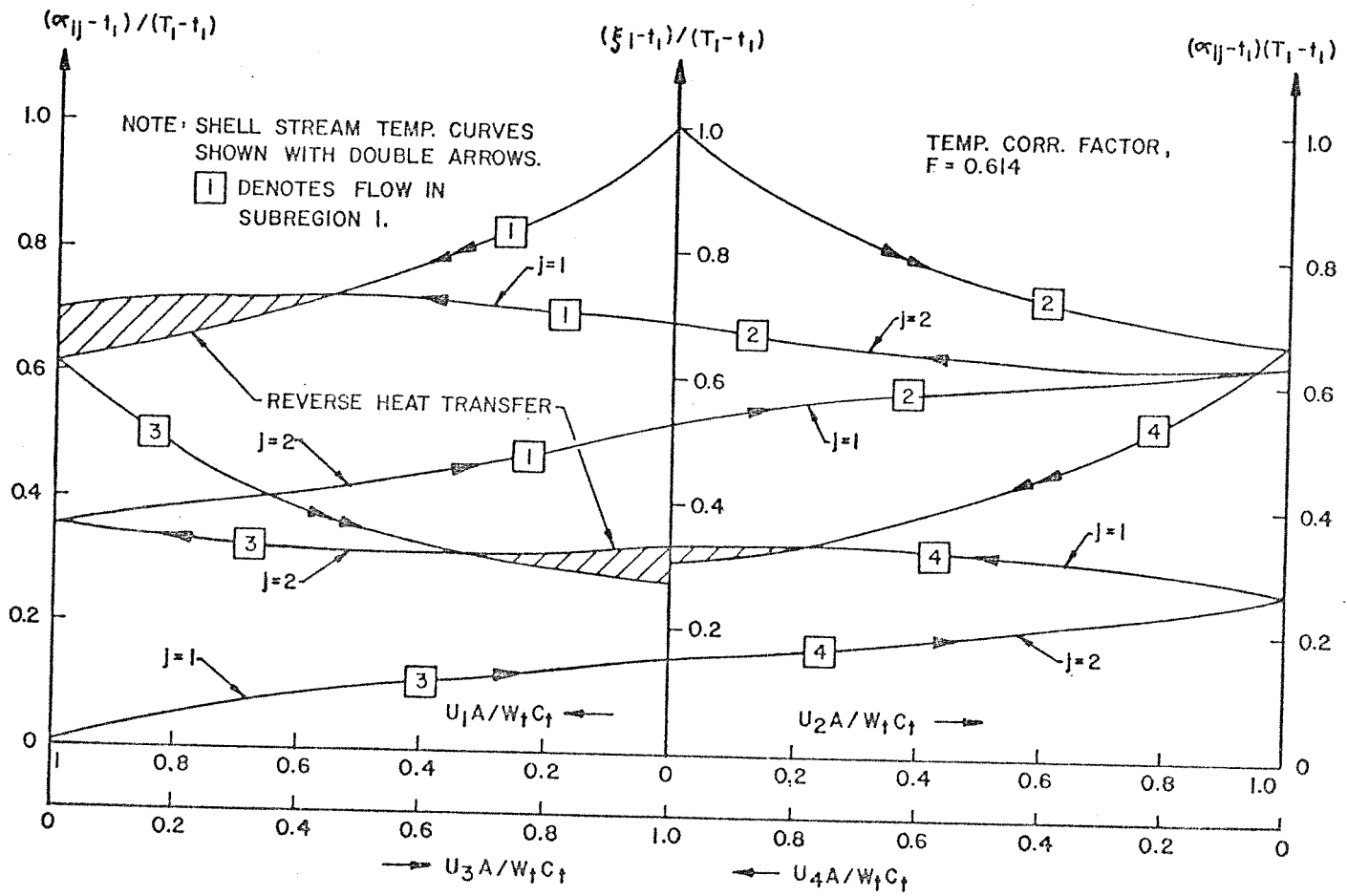

Fig. 5. Temperature profile in a split flow—(4) tube pass heat exchanger.